International Journal of Advanced Research in Physical Science (IJARPS)
Volume 5, Issue 8, 2018, PP 17-28
ISSN No. (Online) 2349-7882
www.arcjournals.org

Super Large Aperture Molecular Lasers

Victor V. Apollonov

Prokhorov GPI RAS, Vavilova 38, 119991, Moscow, Russia

***Corresponding Author:** **Victor V. Apollonov,** Prokhorov GPI RAS, Vavilova 38, 119991, Moscow, Russia*

Abstract: *An excitation of super large aperture CO_2- and N_2O-lasers places demanding and unusual constraints on the pulsed power supply. Stable discharges with interelectrode gaps as large as g >70 cm were achieved [1, 2] using pulsed power supplies [3] that satisfy specific requirements imposed by volume preionization and discharge ignition. The supply must initially apply a quasi-dc or slow-rise voltage to effect preliminary filling of the gap with electrons from an auxiliary discharge, followed by application of a controlled rise voltage to ignite a self-sustained volume discharge (SSVD). A coupled particle kinetics-equivalent circuit model has been developed to simulate discharge behavior for the various pulsed power configurations. Our computational results are compared with experiments involving super large aperture, huge volume devices [1-4].*

1. VOLTAGE WAVEFORMS FOR SSVD INITIATION

1.1. Single-Pulse Waveforms

Three types of voltage waveforms have been used to establish SSVD in CO_2-laser gas mixtures that are preionized by auxiliary discharges. As illustrated by the waveform shown in Fig. la, the first method uses a continuously increasing applied voltage (rise time t_r) to sweep electrons generated by the auxiliary discharge across the main transverse gap and to ignite the discharge. The induced electron drift velocity is zero when the auxiliary discharge is initially fired and then increases as the voltage applied across the main gap $U_d(t)$ rises. Preliminary filling should be complete before discharge ignition [5, *6*], which requires that

$$t_r \geq (3/2)t_{dr} \cong \frac{9g^2}{4\mu_e U_{pk}}. \quad (1)$$

Here t_{dr} is the characteristic drift time, μ_e is the electron mobility, and U_{pk} is the peak discharge voltage.

The second method, as illustrated by the waveform in Fig. 1b, involves the application of a quasi-dc bias voltage U_{bias} for a duration which approximates or exceeds t_{dr}, i.e.,

$$t_{\text{bias}} \geq t_{dr} = \frac{g^2}{\mu_e U_{\text{bias}}}. \quad (2)$$

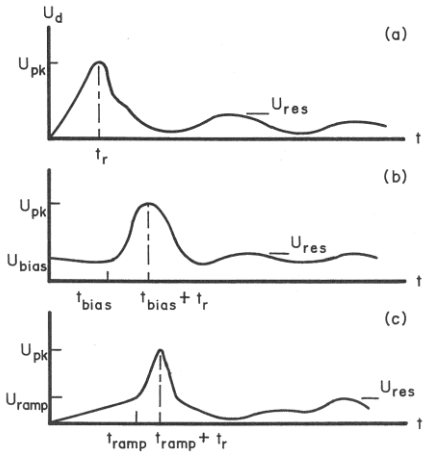

Figla-c. *Voltage waveforms for single-pulse excitation: **(a)** smoothly rising leading edge, **(b)** smoothly rising leading edge with preapplied quasi-dc bias, and (c) ramped bias voltage followed by smoothly rising leading edge [3].*

The value chosen for the quasi-dc bias field, $E_{bias} = U_{bias}/g$, must be large enough to transport electrons across the gap in a reasonably short time but small enough to avoid operation in an E/N regime where losses due to dissociative attachment are a problem. The preionization phase is followed by a gradually rising voltage to ignite the discharge. Sensible current begins to flow across the main gap at or just prior to the time of maximum applied voltage. The voltage rise time is again defined as t_r and its value must be of sufficient duration to avoid premature depletion of the cathode space-charge layer during ignition; hence, there is a maximum rate of voltage rise,

$$\left.\frac{dU_d}{dt}\right|_{max} = f(\text{gas composition}, P, J_{aux}), \tag{3}$$

that should not be exceeded. P is the total gas pressure, and J_{aux} is the current density produced by the auxiliary discharge for a duration t_{aux}. This method can lead to problems if the space-charge screen is suddenly depleted during commutation of the U_{bias} potential; this phenomenon occurs if the condition

$$E_{cf} << E_{bias} \tag{4}$$

is violated, where E_{cf} is the field associated with the cathode fall. Condition (4) can be satisfied if U_{bias} is sufficiently small (which may not be practical) or if the auxiliary discharge is fired prior to commutation of U_{bias}.

The third method uses a slowly increasing ramp voltage waveform to transport the preionizing electrons across the interelectrode gap, followed by a more steeply increasing voltage to ignite the discharge (Fig. lc). The voltage initially increases from zero to U_{ramp} at $t = t_{ramp}$ and then increases more abruptly to U_{pk} over a duration t_r. This method avoids those problems associated with sudden application of a quasi-dc bias at $t = 0$.

1.2. Double-Pulse Waveforms

With this method, any of the three waveform types described previously in Sect. 1.1 is used to establish a low-current, quiescent SSVD. This plasma acts as a prepared load for discharge of a second, fast pulse power supply. The fast pulse circuit is optimized for maximum electrical efficiency.

1.3. Minimum Ignition Voltage

A necessary but insufficient condition for discharge stability is

$$U_{pk} \geq \zeta U_{sb}, \tag{5}$$

where $U_{sb}(E_{sb})$ is the self-breakdown voltage (field) for unprofiled electrodes. U_{sb} is roughly half the self breakdown value measured for profiled electrodes having a uniform electric-field distribution. The factor ζ is stipulated differently depending upon the particular citation: ζ = 1.8 for g < 10 cm [7] and ζ ~ 1.1-1.3 for g = 20-60 cm [3]. Operation with $U_{pk} < \zeta U_{sb}$ causes arcs that occur shortly after the time of voltage maximum if the auxiliary discharge is on, and during the voltage rise if the auxiliary discharge is off or if $t_{aux} < t_r$.

2. COUPLED PARTICLE KINETICS EQUIVALENT CIRCUIT

The behavior of a pulse forming network (PFN) that provides the requisite voltage waveforms can be predicted by modeling the equivalent circuit shown in Fig. 2. The constitutive equations for circuit voltages and currents are

$$\frac{dU_1}{dt} = -\frac{I_1}{C_1}, \tag{6}$$

$$\frac{dU_2}{dt} = -\frac{I_1 - I_2}{C_2}, \tag{7}$$

$$\frac{dU_3}{dt} = -\frac{I_3}{C_3}, \tag{8}$$

$$\frac{dI_1}{dt} = \frac{U_1 - R_1 I_1 - U_2}{L_1}, \tag{9}$$

$$\frac{dI_2}{dt} = \frac{U_2 - R_2 I_2 - U_d}{L_2}, \tag{10}$$

$$\frac{dI_3}{dt} = \frac{U_3 - R_3 I_3 - U_d}{L_3}. \tag{11}$$

The prolonged voltage rise necessary for dynamic profiling of the electric field is produced by the PFN which consists of capacitors C_1 and C_2 and inductors L_1 and L_2. R_1 and R_2 represent resistive losses associated with the transmission lines and switchgear. Switch S_1 is commuted at $t = 0$ which initiates discharge of energy-storage capacitor C_1. A second, fast rise-time voltage is superimposed upon the transverse gap at a later time by commuting switch S_2 at $t = t_f$. This initiates discharge of energy-storage capacitor C_3. R_3 represents resistive line and switch losses and resistor R_4 is necessary to ensure reproducible switch closure and to partially reduce circuit ringing. These equations must be solved simultaneously with equations describing the electron, negative-ion, and N_2, metastable densities:

$$\frac{dn_e}{dt} = (\bar{k}_i - \bar{k}_a) n_e N - k_r^{ei} n_e n_+ + \bar{k}_d n_- N + \frac{n_m}{\tau_p}, \tag{12}$$

$$\frac{dn_-}{dt} = \bar{k}_a n_e N - \bar{k}_d n_- N - k_r^{ii} n_+ n_-, \tag{13}$$

$$\frac{dn_m}{dt} = k_m n_e [N_2] - \frac{n_m}{\bar{\tau}}, \tag{14}$$

where n represents particle concentration (particles/cm^3) and the subscripts e, +, —, and m denote electrons, positive ions, negative ions, and metastable species, respectively. Processes (and rate coefficients) include primary electron-impact ionization (k_i), electron attachment (k_a), electron detachment (k_d), electron-ion recombination (k_r^{ei}), ion-ion recombination (k_r^{ii}), and N_2 a-state excitation (k_m). The bar notation indicates rate coefficients which are weighted for the particular gas mixture and which are functions of the local value of the reduced electric field E/N, where N is the total particle concentration. [N_2] is the nitrogen gas concentration (constant). $\bar{\tau}$ is the characteristic time for collisional deactivation of the metastable level (weighted for the particular gas mixture) and τ_p is the characteristic time for Penning collisions; $1/\tau_p = k_p N_{ri}$, where N_{ri} is the concentration of readily ionizable molecules such as tri-n-propylamine (TPA). The positive-ion density is found by assuming charge neutrality in the positive column:

$$n_+ = n_e + n_-. \tag{15}$$

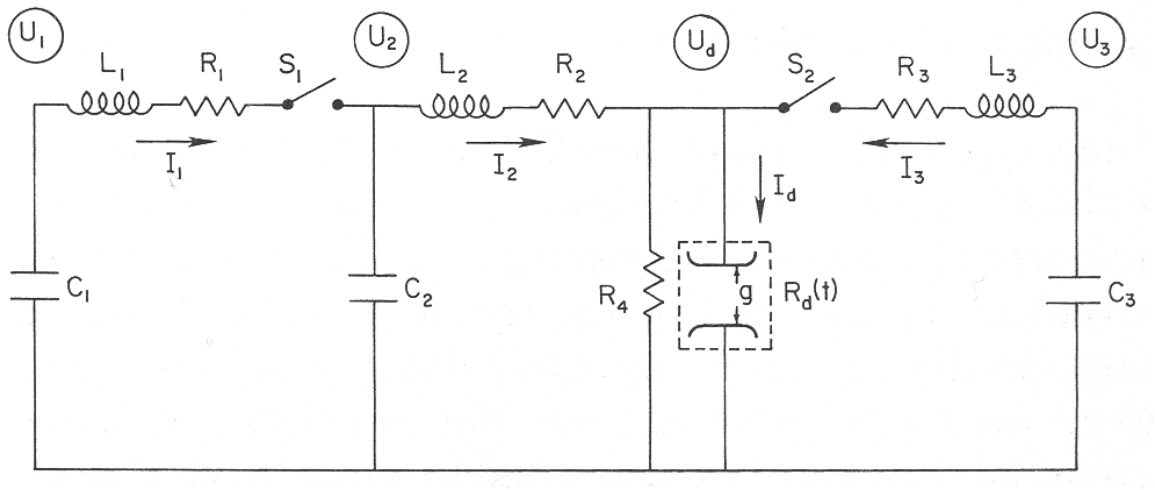

Fig2. *Equivalent-circuit schematic diagram*

The initial conditions for the system of ordinary differential equations (ODEs) are

$$U_1(0) = U_c, \tag{16}$$

$$U_2(0) = U_d(0) = U_{\text{bias}}, \tag{17}$$

$$U_3(0) = U'_c, \tag{18}$$

$$I_1(0) = I_3(0) = I_d(0) = 0, \tag{19}$$

$$I_2(0) = U_{\text{bias}} / R_4, \tag{20}$$

$$n_e(0) = n_{e0}, \tag{21}$$

and

$$n_-(0) = n_m(0) = 0, \tag{22}$$

where U_e is the charging voltage on capacitor C_1, U'_e is the charging voltage on capacitor C_3, and n_{e0} is the initial electron density. U_{bias} is the quasi-dc bias voltage applied to the gap prior to closure of either switch or S_2. If $U_{\text{bias}} > 0$, then a quasi-dc field was used to sweep preionizing electrons across the interelectrode gap and the initial potentials on capacitor C_2 and the discharge gap are equal to U_{bias}. The duration of this preionization process ($\sim t_{dr}$) does not enter into the present model since we assume that the entire interelectrode gap is uniformly filled with electrons with density n_{e0} at $t = 0$. The discharge voltage and current are

$$U_d(t) = \frac{I_2 R_4 R_d}{R_4 + R_d} \tag{23}$$

and

$$I_d(t) = I_2 - \frac{U_d}{R_4}. \tag{24}$$

The discharge resistance is related to the electron density by

$$R_d(t) = \frac{g}{e\mu_e n_e A}, \tag{25}$$

where e is the electronic charge and A is the effective discharge area. The contribution to plasma conductivity by positive- and negative-ion species is small and is neglected in (25). Because

$\mu_e = \mu_e(E/N)$, (25) must be solved iteratively and self-consistently along with (6-15). The bias voltage, if nonzero, is small enough that the discharge gap is initially non-conductive, i.e., $R_d(0) >> R_4$. The instantaneous power supplied to the discharge is

$$P_d(t) = U_d(t) I_d(t), \tag{26}$$

the energy dissipated in the discharge is

$$E_d = \int P_d(t) dt, \tag{27}$$

the electrical efficiency is

$$\eta_{e1} = 2E_d / (C_1 U_e^2 + C_2 U_{\text{bias}}^2 + C_3 U'^2_e, \tag{28}$$

and the specific input energy is

$$\xi_i = E_d / V, \tag{29}$$

where V is the disharge volume.

With this model, we have the option of simulating either double-pulse excitation using the entire circuit or single-pulse excitation using the reduced-form equivalent circuit (by setting $t_f = \infty$). The system of differential equations was coded for computer solution using a robust ODE solver (LSODE from the Lawrence Livermore ODEPACK collection [*8*]). Rate and transport coefficients were determined separately by solution of the Boltzmann equation at tabulated values of *E/N* and then determined within the code using a fourth-order (cubic) Lagrangian interpolator [5].

3. PULSED POWER SYSTEMS

Both Marx [3, 9] and Fitch-Howell [3, 10] pulse generators, with suitable modifications, have been used to produce the waveform types shown in Fig. 1. The equivalent circuit in the present model (Fig. *2*) is applicable only to the former system. To produce the voltage waveform with a smoothly rising leading edge (Fig. la), the PFN parameters are adjusted so that

$$t_r \approx \pi \left(\frac{L_1 C_1}{4} \right)^{1/2}, \tag{30}$$

where $C_1 = C/N_s$ is the equivalent Marx bank capacitance, C is the capacitance of each stage, and N_s is the number of stages. The equivalent charging voltage is then $U_c = N_s U_a$, where U_a is the actual generator charging voltage. The approach in [3] typically use $C_2 = C/N_s$, so the discharge current period is

$$T \approx 2\pi (L_2 C_2)^{1/2}. \tag{31}$$

The voltage waveform with a quasi-dc bias (Fig. lb) is produced simply by charging capacitor C_2 to voltage U_{bias} and inserting the main switch between C_2 and the discharge. No isolation switch is necessary between the Marx bank and C_2 if $U_{\text{bias}} = U_a$. The voltage waveform with an initial ramp to U_{ramp} (Fig. lc) is produced by substituting a two-stage *LC* circuit for the single capacitor C_2.

4. COMPUTATIONAL RESULTS

4.1. Single-Pulse Excitation Without Quasi-dc Bias

The rise time t_r (cf. Fig. la) is adjusted by varying the ratio of PFN inductances, here expressed by the dimensionless parameter

$$M = \frac{L_1}{L_2}. \tag{32,33}$$

I_{pk} is the peak current which occurs at time t_{pk} and t_{qs} is defined by the full width at half maximum (FWHM) current pulse width. In this example, Q = 0.61, E_{qs}= 10 kV/cm, I_{pk} = 13 kA, t_{qs} = 0.8 μ s, η_{e1} = 66%, and ξ_i = 297 J/l.

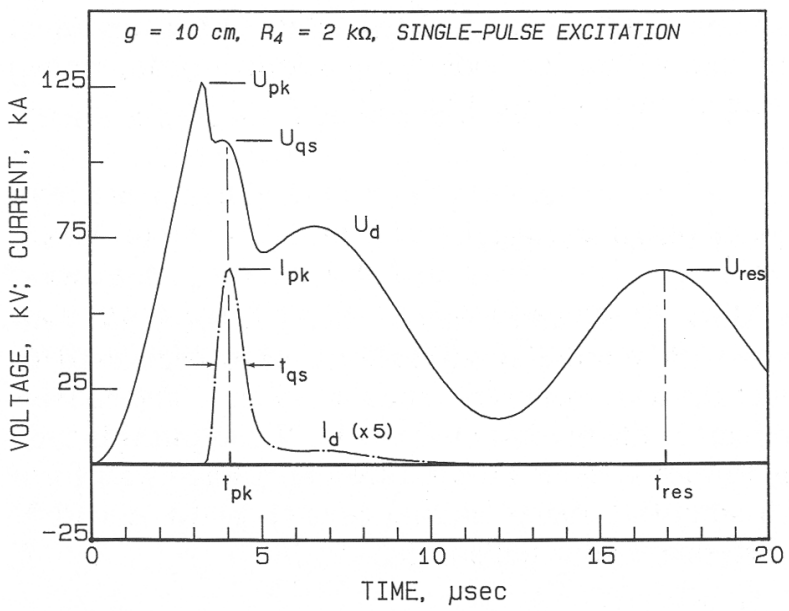

Fig3. *Representative* I_d — U_d *waveforms for single-pulse excitation and definition of nomenclature.*

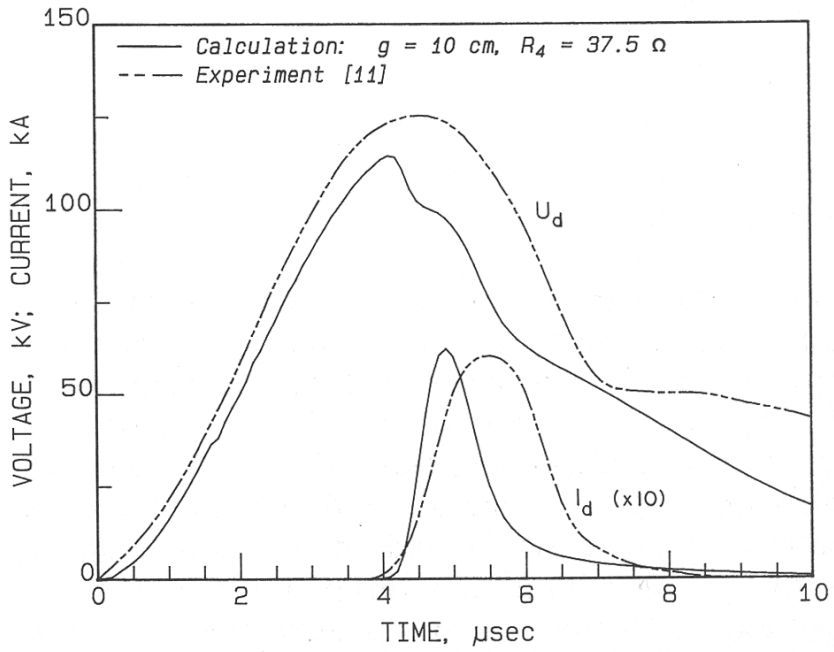

Fig4. *Computed and measured* I_d — U_d *waveforms for the device described in [11]*

U_{res} can be reduced by decreasing the parallel resistance R_4, but this occurs at the expense of reduced electrical efficiency. For example, the device in [11] employed a CO_2:N_2:He = l:4:5 gas mixture at atmospheric pressure with g = 10 cm and A = 400 cm^2. Stated circuit parameters were C_1 =0.25 μF, C_2 = 0.1 μF, U_c = 120 κV, L_1 ~ 15-20 μH, L_2 ~ l μH, and $R_4 = 75/N_r$ Ω, where N_R is an unspecified number of resistors in parallel. The small value of R_4 helps to prevent discharge voltage ringing and arc formation after the glow period. The choice of N_R strongly effects the computed value of I_{pk} and N_R = 2 gave the best agreement with experiment. Assumed parameters were R_1=R_2 = 10 mQ, n_{e0} = 10^7 cm^{-3}, and P_{ri} = 0.75 Torr (TPA). Computations performed with these parameters gave values of t_r and t_{pk} which were too short, indicating that M was too small. By increasing to 35 μF (i.e., M = 35), voltage and current waveforms (Fig. 4) were obtained in approximate qualitative and quantitative agreement with measurements (the computations depicted in Figs. 3 and 4 are therefore identical with the exception of R_4). The principal discrepancy is between the computed (t_{qs} = 0.9 μs)

and experimental (t_{qs} = 1.4 μs) current pulse widths, which is probably related to two-dimensional effects such as the current density distribution across the electrodes. This circuit is poorly designed, viz., η_{e1} = 34% and ξ_i = 153 J/l. The importance of Penning ionization of the readily ionizable additive is illustrated by a computational experiment with the N_2 metastable kinetics turned off. In this case, I_{pk}<2 kA.

It is useful to examine parametric regions where Q can be maintained below a specified minimum, i.e., $Q < Q_{min}$. For each value of Q_{min} there exists an $M_{max} = M(Q_{min})$ at which it is still possible to obtain $Q < Q_{min}$. In the paper [9] found that M_{max} is only weakly dependent upon L_1, L_2, $C_1 = C_2$, g, A or n_{e0}. Concurrently, there exists a maximum value of t_r for each Q_{min}, $t_{r,max}$, given by

$$t_{r,\max}(Q_{\min}) = \pi\left(\frac{L_2 C_1 M_{\max}}{4}\right)^{1/2}. \tag{34}$$

$t_{r,max}$ can be increased by increasing inductance L_2, but this also increases the discharge current pulse width. The duration of the SSVD can be crudely bounded by the duration of the discharge half-period [cf. (31)], i.e.,

$$t_{qs} \geq T_{1/2} = \pi(L_2 C_2)^{1/2}. \tag{35}$$

Combining (34) and (35) yields the condition

$$t_{r,\max} \leq t_{qs}\left(\frac{M_{\max}}{4}\right)^{1/2}. \tag{36}$$

Thus, the maximum voltage rise time is limited by the requirement to deposit energy into the SSVD efficiently. The maximum permissible discharge gap can be estimated from the requirement for complete electron filling during the preionization phase as discussed previously, hence

$$g_{\max} \cong (0.3-0.4)\mu_e t_{r,\max} U_c / g, \tag{37}$$

where the numerical factor arises from the necessity to complete the preliminary filling process prior to discharge ignition. If we desire t_{qs} = 5 μs and Q_{min} = 0.3, then $t_{r,max}$ ~ 15 μs. Using representative values of μ_e = 10^3 cm^2/V-s and U_c/g ~ $2U_{qs}/g$ = 10 kV/cm, we obtain g_{max} = 40-50 cm for atmospheric-pressure operation. The largest experimental values of g for this type of excitation are indeed comparable to this estimate [1-3]. Arc free SSVD in a 60-cm gap could only be obtained with a 50% probability by means of single-pulse excitation [1]. Note that (37) applies only for single pulse excitation without quasi-dc bias.

4.2. Single-Pulse Excitation With Quasi-dc Bias

In this type of excitation, the processes of preionization and discharge ignition are separate (cf. Fig. lb) and there is no maximum rise-time condition analogous to (34). Instead, there exists a maximum rate of voltage rise $dU_d/dt|_{max}$ which produces consequential depletion of the negative space-charge layer covering the cathode. Operation with $dU_d/dt > dU_d/dt|_{max}$ spoils the dynamic profiling process [cf. (3)] and reduces the probability for establishing a stable, homogeneous SSVD. For auxiliary barrier discharges, $dU_d/dt|_{max}$ ~ 10 kV/μs [9]. By replacing the auxiliary barrier discharge with an auxiliary surface discharge, the maximum rate of voltage rise could be increased to $dU_d/dt|_{max}$ ~ 30-40 kV/μs [2]. This attests to a higher productivity (larger J_{aux}) by the surface discharge and allows a decrease in t_r.

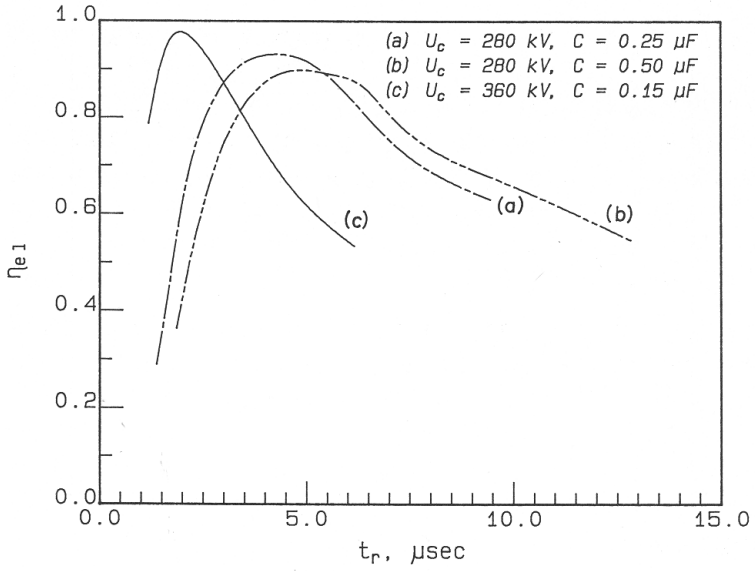

Fig5. *Computed dependence of the electrical efficiency* η_{e1} *on the voltage rise time* t_r.

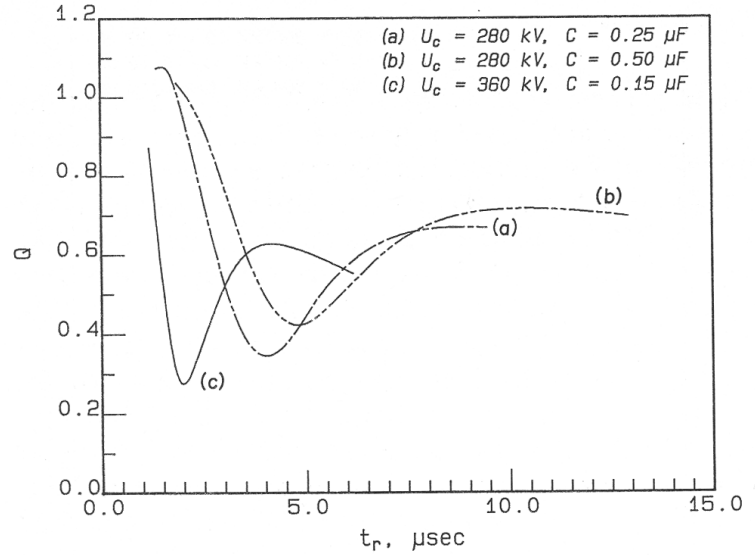

Fig6. *Dependence of the dimensionless parameter* Q *on the voltage rise time* t_r.

Table1. *Computational parameters for single-pulse excitation with dc bias*

Circuit parameters	Case (a)	Case (b)	Case (c)
C_1; C_2 [μF]	0.25	0.50	0.15
L_1[μH]	ML_2	ML_2	ML_2
L_2[μH]	2.0	2.0	2.0
R_1;R_2 [Ω]	0.01	0.01	0.01
R_4[Ω]	2000	2000	2000
U_c [kV]	280	280	360
U_{bias} [kV]	56	56	72
E_s/V[J/1]	200	400	200
Geometry and initial conditions Gas mixture			
g[cm]	25	CO2: N2:He	1:4:5
A[cm^2]	2000	Pri[Torr] (TPA)	0.75
V[1]	50	P[Torr]	750
Neo [cm^{-3}]	107	T [K]	293

The current-voltage characteristics of a 50-1 device were numerically simulated to better understand the electrical design constraints that accompany this type of excitation. The parameters chosen for three cases are listed in Table 1 and would be typical of a 5-stage Marx bank. Case (a) is described by

$E_s/V \equiv \xi_i/\eta_{el} = 200$ J/l (i.e., ideal operation of this circuit would produce a specific input energy of 200 J/l) and by a peak discharge voltage which is above the ignition threshold but below the value for impedance matching. By varying L_1 from 2 to 200 μH (M = *1* to *100*), t_r can be adjusted over about an order of magnitude. Computational results clearly show that although the discharge efficiency η_{e1} initially increases with increasing rise time (Fig. 5), circuit ringing is a persistent problem and no value of M produces $Q < 0.3$ (Fig. *6*). t_{qs} increases gradually as a function of t_r and approaches the asymptote $T_{1/2} = 2.2$ μs. I_{pk} increases rapidly with t_r, reaches a maximum at $t_r \sim 3$ μs ($I_{pk} = 33$ kA), and then decreases gradually. The minimum degree of circuit ringing (Q = 0.34) and the maximum electrical efficiency (η_{e1} = 93%) occur simultaneously at $t_r = 4$ μs ($M = 13$). However, operation with such a short value of t_r yields a rate of voltage rise, $dU_d/dt \sim (U_{pk} - U_{bias})/ t_r = 40$ kV/μs, which is probably too large. If M and thus t_r are adjusted to reduce the maximum rate of voltage rise to $dU_d/dt < 10$ kV/μs, then the large residual voltage amplitude ($Q > 0.6$) will invite arc formation at $t = t_{res}$.

Case (b) is identical to (a) with only a doubling in the capacitances C_1 and C_2 (i.e., $E_s/V \equiv \xi_i/\eta_{e1} =$ 400 J/l, which may be above the maximum for this gas mixture and type of excitation). Since $I_{pk} \propto (C_2/L_2)^{1/2}$ and $t_{pk} \propto (C_1/L_1)^{1/2}$, both parameters are characteristically larger in the present case, but discharge ringing is not alleviated. The minimum degree of circuit ringing ($Q = 0.42$) and the maximum electrical efficiency (η_{e1} = 89%) occur simultaneously at $t_r = 5$ μs ($M = 13$). Again, however, such a large rate of voltage rise ($dU_d/dt \sim 30$ kV/μs) may preclude satisfactory operation at this value of t_r.

All of the energy stored in the PFN is deposited into the laser discharge in the first cycle of operation if their impedances are matched. Since the laser discharge is effectively a constant voltage load, this occurs only if

$$U_c \cong 2U_{qs}. \tag{38}$$

Case (c) maintains $E_s/V \equiv \xi_i/\eta_{e1} =$ 200 J/1 as in case (a) but increases the charging voltage to $U_c =$ 360 kV in conformance with this condition. C_1 and C_2 are decreased accordingly. Optimization of the circuit is now possible with marked improvement in current-voltage characteristics. Minimum circuit ringing ($Q = 0.28$) and maximum electrical efficiency (η_{e1} = 98%) occur concurrently at $t_r = 2.0$ μs. The glow duration ($t_{qs} = 1.3$ μs) is now approximately the same as in the previous cases and the peak current ($I_{pk} = 44$ kA) is approximately equal to the maximum encountered with case (b). Note that a value of $Q \sim 0$ is not obtained because (38) is valid only if $C_1 = C_2$ and $U_{bias} = 0$. While the optimization described here appears to adjacent to the cathode is not depleted. After establishment of the quiescent SSVD, additional energy can be rapidly loaded without disruption of plasma homogeneity or stability [*1*, *2*].

To achieve a deliberately prolonged rise time for practical devices, however, it is often necessary to increase M to a value for which impedance matching between the PFN and load is poor. Typically, the PFN impedance is larger than the load (laser discharge) and the voltage waveform oscillates as shown by the example in Fig. 3. This computation was performed for a small ($g = 10$ cm, A =400 cm^2), atmospheric-pressure ($CO_2:N_2:He = 1:4:5$) device with electrical parameters C_1 =0.25 μF, C_2 = 0.1 μF, U_c = 120 kV, L_1 = 35 μH, L_2 = l μH, $R_1 = R_2 = 10$ mΩ, $R_4 = 2$ kΩ; also, $n_{e0} = 10$ cm^{-3} and P_{ri} = 0.75 Torr (TPA). If U_{res} is defined as the amplitude of the second or *residual* voltage peak which occurs at time t_{res} and if U_{qs} is defined as the discharge voltage at peak discharge current, then it is useful to find the electrical circuit parameters which minimize the dimensionless parameter

$$Q = \frac{U_{res}}{U_{qs}}.$$

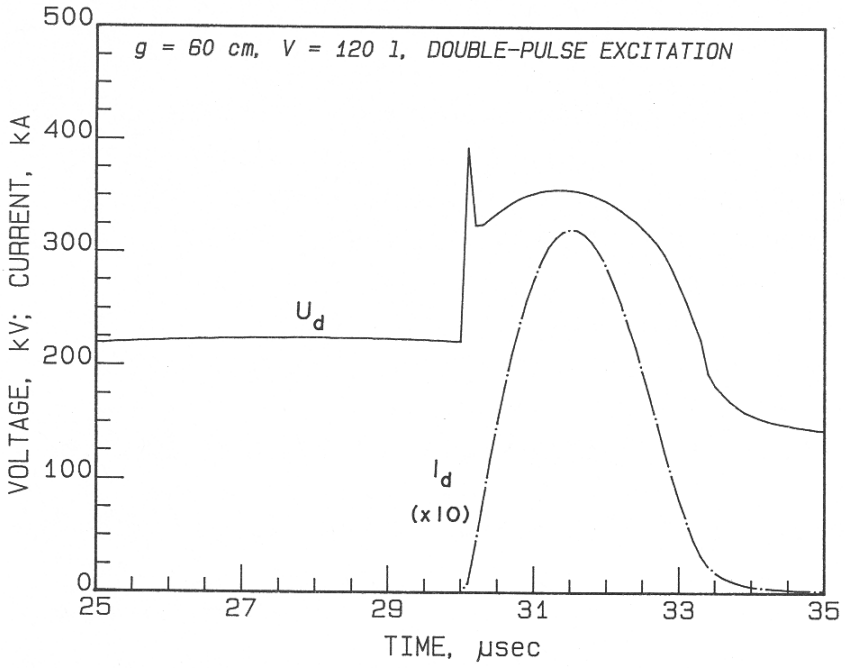

Fig7. *Computed* I_d—U_d *waveforms for double-pulse excitation of the device described in [1]*

Waveforms for single- and double pulse excitation of a 60-cm aperture, 120-1 device are given in [1]. The atmospheric-pressure gas mixture (CO_2:N_2:He = 4:16:80) was preionized by an auxiliary barrier discharge attached to the top surface of the cathode. Explicit PFN parameters are not given. For the double-pulse computation, therefore, numerical simulations were performed to find electrical parameters which would produce a quiescent plasma having an electron concentration $n_e \sim 10^{10}$ cm^{-3} at the conclusion of a slowly rising voltage pulse of duration

$$t_r \approx \frac{9g^2}{4\mu_e U_e (C_1/C_2)^{1/2}}. \tag{39}$$

Then at $t_f = t_r$, switch S_2 is closed, depositing ~ 200 J/l into the plasma in accordance with impedance-matching condition 138). To yield these results, a double-pulse PFN was designed with electrical parameters C_1 = 0.2 μF, C_2 = 0.1 μF, C_3 = 0.2 μF, L_1 = 1200 μH, L_2 = 100 μH, L_3 = 5 μH, R_1 = R_2 = R_3 = 10 mΩ, R_4 = 5 kΩ, U_c = 180 kV, U_{bias}=45 kV, U'$_c$ = 520 kV; also, n_{e0}= 5x10^6 cm^{-3} and P_{ri} = 1.5 Torr. Closure of switch S_1 produces a gradual increase in U_d to 220 kV over a duration t_r=30 μs, generating a current flow of only I_d ~ 10 A. Note that this PFN is designed as a voltage multiplier (i.e., $C_1 > C_2$) so that $U_d(t_r) > \zeta U_{sb}$ even though $U_c < \zeta U_{sb}$. The PFN that consists of capacitors C_1 and C_2 and inductors L_1 and L_2 is effectively isolated from the second discharge pulse produced by the L_3 — C_3 PFN provided that $L_2 >> L_3$. Furthermore, the stored energy for the first pulse is only 12% of that for the second, main pulse. Computed I_d — U_d waveforms for the time interval encompassing the second pulse are shown in Fig. 7.

Table2. *Comparison of computed and experimental discharge parameters for double-pulse excitation of a 120-1 device*

Parameter	Experiment [1]	Computation
tr [μS]	≈ 30-45	30
U d(tr) [kV]	240	221
ne (tr) [cm -3]	--	9x1010
Upk [kV]	≈ 380	393
U qs [kV]	≈ 290	355
tqs [μS]	≈ 3	2.1
Ipk [kA]	42	32.1
ζi [J/1]	≃ 180	188
η_{el}	≃ 0.90	0.74

Measured and computed discharge parameters are listed in Table 2. This type of excitation produces a shorter-duration, higher-current SSVD than possible with single-pulse excitation in qualitative agreement with experiment. The computed values of U_{qs} and I_{pk} are respectively larger and smaller than the experimental measurements, but the agreement between ξ_i values is excellent. Furthermore, it is now possible to vary t_{qs} and therefore I_{pk} by adjusting L_3 without sacrificing electrical efficiency. The simulation here showed little circuit oscillation beyond the first cycle (i.e., $Q < 0.1$).

A 140-1 device with a 70-cm interelectrode gap is described in [2]. This device employed an auxiliary surface discharge that was placed beneath the mesh cathode. The cathode was operated at ground potential and the auxiliary discharge was fed by a separate pulsed- power system. Electrons were repelled from the surface-discharge plasma and through the grid by applying a negative bias voltage to the auxiliary-discharge circuit. VUV radiation is only produced during the breakdown process for this type of auxiliary discharge whereas electrons can be extracted during the entire duration t_{aux}. PFN parameters are not given and the I_d — U_d waveforms are described as being qualitatively similar to those in [1]. For the present simulation, PFN parameters that initially establish a quiescent SSVD were again chosen by trial and error. The second, high-current discharge then operates according to impedance matching condition (38). The interelectrode gap is filled both by an initial burst of photoelectrons produced by surface-discharge VUV radiation and from electrons extracted from the surface-discharge plasma during the entire quiescent period. The computed specific input energy (ξ_i = 130 J/l) is in good agreement with experiment (ξ_i = 140 J/l) and the computed electrical efficiency is quite have alleviated the impedance matching problem, the large rate of voltage rise (dU_d/dt ~ 100 kV/μ s) will certainly destroy the cathode space-charge screen for even the highest productivity auxiliary discharges. Establishment of a stable SSVD under these conditions is highly unlikely.

4.3. Double-Pulse Excitation

This type of excitation is produced by firing the left-hand PFN (switch S_1) at decreased charging voltage and stored energy, which produces a slowly increasing discharge voltage waveform and establishes a low-current but stable SSVD, followed by commutation of switch S_2, which dumps the main energy store (capacitor C_3 charged to voltage U'_c) into the plasma. The advantage here is that the SSVD is established under *low- dU_d/dt* conditions and the negative space-charge layer high (η_{e1} = 80%).

5. CONCLUSIONS

Computational runs using a coupled particle kinetics equivalent circuit model were performed to simulate response of the various PFNs that are used with the auxiliary discharge excitation scheme. A single pulse PFN, with or without quasi-dc bias, can only be employed with q < 40-50 cm, in excellent agreement with experimental findings. This limitation is imposed by design conflicts between the need for increasingly longer rise times as the gap is increased and the requirement for impedance matching between the PFN and discharge plasma load. Larger discharge gaps require more complex circuitry to first establish a low-current, quiescent SSVD using a slow rise time initial pulse, followed by a second high current, fast rise time pulse that deposits the bulk of the stored energy into the discharge plasma of super large aperture molecular lasers [12-14].

REFERENCES

[1] V.V. Apollonov, G.G. Baitsur, A.M. Prokhorov et al, Sov. Tech. Phys. Lett. 14, 241-242 (1988)

[2] V.V. Apollonov et al, Sov. Tech. Phys. Lett. 14, 915, (1988)

[3] V.V. Apollonov et al, Instrum. Exp. Technol. 32, 149, (1989)

[4] V.V. Apollonov et al, Ultraviolet preionized SSVD in a volume of 400 liters, paper scheduled for presentation at Pulse Power for Lasers, Proc. SPIE 1411,(1991)

[5] V.V. Apollonov et al, J.Opt.Soc.Am.B,V.8, N2, (1991)

[6] V.V. Apollonov et al, Enhanced transverse discharge stability using preionization from an auxiliary barrier discharge, Proc. of the conference: Seventh Intern. Symp. on Gas Flow and Chemical Lasers, 58, (1989)

[7] V.V. Apollonov et al, Sov. J. Quantum Electron. 17, 76 (1987)

[8] A.C. Hindmarsh: In Scientific Computing, ed. by R.S. Stepleman (North-Holland, Amsterdam 1983) pp. 55-64 A.C. Hindmarsh: Lawrence Livermore National Laboratory, private communication (1990)

[9] V.V. Apollonov, Small signal gain of CO2-lasers pumped by SSVD, International conf. on Lasers-87, Lake Tahoe, 495, (1987)

[10] R.A. Fitch, V.T.S. Howell: Proc. IEE 111, 849, (1964)

[11] V.V. Apollonov et al, Sov. J. Quantum Electron. 15, 1, (1985).

[12] V.V. Apollonov, High power molecular lasers pumped by a self-controlled volume discharge, J. Opt. Soc. Am. B, Opt. Phys. 8, 2, 220, (1991)

[13] V.V. Apollonov, High power self-controlled volume discharge based molecular lasers, Opt. Eng. 43 (1), (2004)

[14] V.V. Apollonov, High power/energy molecular lasers, SPRINGER (2016)

Citation: *V. Apollonov, "Super Large Aperture Molecular Lasers", International Journal of Advanced Research in Physical Science (IJARPS), vol. 5, no. 8, pp. 17-28, 2018.*